High-order numerics for simulating turbulent deflagration fronts over coarse meshes

Eurielle Bossennec, Guido Lodato, Luc Vervisch
Normandie Univ., INSA de Rouen Normandie, CORIA, CNRS
76000 Rouen, France

1 Introduction

The accurate control of the spatial resolution of scalars involved in the description of turbulent flame fronts is at the core of many issues faced when simulating turbulent flames. This is specifically the case in large-eddy simulation (LES) where only the largest flow scales are resolved. In zones where the mesh is coarse, the bounded character of the scalar is not always preserved by the numerical scheme without adding some amount of artificial diffusivity to make the signal thicker. In the artificially thickened flame approach [1], the boost in diffusivity is designed to preserve major flame properties.

Modern high-order methods are grounded on high-order polynomial approximations of the scalar fields [2–4]. Along these lines, using a modal decomposition of the chemical source for reactive scalars, a sensor constructed from the modal decay rate of the polynomial approximation of the chemical source allows for automatically locating flow zones where the mesh resolution is too coarse for the flame signal (i.e. source terms) to be resolved. This sensor is easily related to a thickening factor (based on a boost in scalar diffusivity) in order to calibrate, from a direct treatment of the scalar signals seen in the simulation, an artificially thickened flame closure.

A similar treatment is applied to the components of the scalar gradients, to calibrate a sub-grid scale flame wrinkling factor from the energy of the modes of the resolved scalar gradient. The method is first applied to one-dimensional flames at various mesh resolutions and orders of discretisation. Then, a three-dimensional canonical turbulent flow is simulated. Starting at a high level of resolution, the mesh is made coarser and statistical results are compared to confirm the validity of the discussed strategy.

2 Numerics and control of chemical source resolution

Recently, several high-order methods have been proposed, including Spectral Difference [2–4] (SD) and Flux Reconstruction [5–7] (FR) type schemes. The SD approach is retained in this study, using a flow solver whose details may be found in [8].

Correspondence to: vervisch@coria.fr

The quality of the resolution of a reactive scalar mainly depends on the quality of the resolution of its source term. Within the SD context, the source term may be reconstructed from a modal decomposition:

$$\dot{\omega}_Y(\xi^i,t) = \sum_{j=1}^{n} \dot{\omega}^{\star}_{Y_j}(t) P_{j-1}(\xi^i) \,, \tag{1}$$

with $\dot{\omega}^{\star}_{Y_j}(t)$ the j-th mode of the scalar source in the direction ξ_k and $P_{j-1}(\xi^i_k)$, the Legendre polynomial of order $j-1$. Because the solution is advanced in time in the code using a nodal decomposition [8], the modes of Eq. (1) are readily obtained from the available nodal values thanks to the inverse Vandermonde matrix [9]. Thereafter a single direction is considered for simplifying the notation, the extension to three dimensions by applying the relation (1) to ξ^i_1, ξ^i_2 and ξ^i_3 is straightforward. Once the modes are known, the method discussed by Persson and Peraire [10, 11], to control the resolution of a signal, is applied to the chemical source. It is based on the idea that for a well resolved signal, the difference between two polynomial approximations of order $n-1$ and n stays small (for n sufficiently large), if not the case then the signal is not properly resolved. The approximation of the solution without the last n-th mode would read:

$$\widehat{\dot{\omega}}_Y(\xi^i,t) = \sum_{j=1}^{n-1} \dot{\omega}^{\star}_{Y_j}(t) P_{j-1}(\xi^i) \,. \tag{2}$$

For well-resolved solutions, hence solutions which are seen as smooth by the mesh, the difference between the two polynomial approximations:

$$\Delta\dot{\omega}_Y(\xi^i,t) = \dot{\omega}_Y(\xi^i,t) - \widehat{\dot{\omega}}_Y(\xi^i,t) = \dot{\omega}^{\star}_{Y_j}(t) P_{n-1}(\xi^i) \,, \tag{3}$$

which is equal to the contribution of the last mode ($j = n = p+1$), is expected to stay very small compared to the sum of the contribution of the other modes ($j = 1, \cdots, p$). A direct measure of the smoothness of the signal within the element (cell) may thus be constructed by comparing the energy of the last mode within the cell to the total energy of the modes:[1]

$$s_{\dot{\omega}_Y} = \log_{10}\left(\frac{\dot{\omega}^{\star 2}_{Y_n}}{\sum_{i=1}^{n} \dot{\omega}^{\star 2}_{Y_i}}\right) \,. \tag{4}$$

In practice $s_{\dot{\omega}_Y}$ is negative and it increases with the relative amplitude of the last mode. The threshold value $s^o_{\dot{\omega}_Y}$ above which the signal is considered as discontinuous, depends on the order of the method and on the distribution used for the solution points (here Gauss-Legendre quadrature points). An auto-calibration strategy of sensors was discussed recently [8]. This method is extended to chemical sources, to define a scalar source-sensor threshold valid for any arbitrarily value of the order of the method. The sensor threshold reads (see Fig. 1):

$$s^o_{\dot{\omega}_Y} = s^{\mathrm{MS}}_{\dot{\omega}_Y} - C_{\mathrm{E}} \,. \tag{5}$$

The constant $C_{\mathrm{E}} = 3$ is a calibration parameter, which does not depend on the order of the numerical method used, as shown thereafter in the one-dimensional flame test case.

Once a discontinuity has been sensed in the chemical source signal, an amount D^{Ad}_Y of additional diffusivity is imposed locally within the element and a flame thickening factor $F(\underline{x},t) = (D_Y + D^{\mathrm{Ad}}_Y(\underline{x},t))/D_Y$ [1] is

[1] The values of the Legendre polynomials P_{j-1} do not enter explicitly the definition of the sensor. Indeed, when the full signal is considered in the analysis via $(\Delta\dot{\omega}_Y(\xi^i,t), \Delta\dot{\omega}_Y(\xi^i,t))_e / (\dot{\omega}_Y(\xi^i,t), \dot{\omega}_Y(\xi^i,t))_e$, the ratio of the standard inner products within the element reduces to Eq. (4), because of the orthogonality of the Legendre basis.

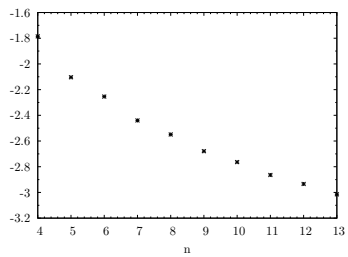

Figure 1: Response of $s^{\mathrm{MS}}_{\dot{\omega}_Y}$ obtained from manufacture solution *vs* order of accuracy $n = p + 1$.

defined to be applied to the scalar equation, where D_Y denotes the diffusivity of the scalar. This diffusivity is calibrated as the additional viscosity discussed in [10]:

$$D_Y^{\mathrm{Ad}} = \begin{cases} 0 & \text{if } s_Y < s_Y^{\mathrm{o}} - \kappa \\ \dfrac{D_Y^{\mathrm{o}}}{2}\left(1 + \sin\dfrac{\pi(s_Y - s_Y^{\mathrm{o}})}{2\kappa}\right) & \text{if } s_Y^{\mathrm{o}} - \kappa \leq s_Y \leq s_Y^{\mathrm{o}} + \kappa \\ D_Y^{\mathrm{o}} & \text{if } s_Y > s_Y^{\mathrm{o}} + \kappa\,, \end{cases} \tag{6}$$

where $\kappa = 1$ determines the width of the transition between no additional diffusivity and its nominal level D_Y^{o}, which is expressed in the fully compressible solver as:

$$D_Y^{\mathrm{o}} = C_D \max(|\mathbf{u}| + c) \times [h/(n-1)]\ , \tag{7}$$

where h is the element size and $C_D = 0.006$ is a pre-multiplier coefficient. $|\mathbf{u}|$ is the velocity magnitude and c is the speed of sound.

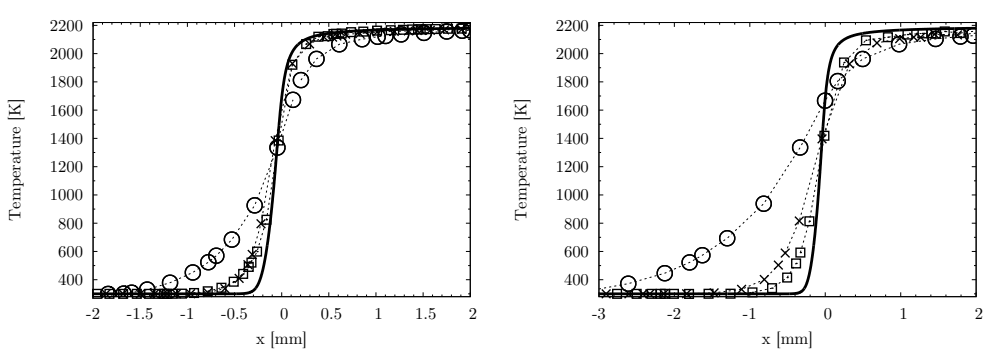

(a) $h = 898\mu\mathrm{m}$ (b) $h = 1795\mu\mathrm{m}$

Figure 2: Temperature distribution in a freely propagating premixed flame. Line: DNS ($h = 15\mu\mathrm{m}$). Circle: 5th order. $\times$: 7th order. Square: 9th order

A similar approach is followed based on the modal decomposition of the scalar gradient $\nabla Y \cdot \vec{\xi}_j$ to define a sensor $s_{\nabla Y}$ in order to calibrate the unresolved SGS wrinkling of a turbulent flame surface, via a SGS wrinkling factor Ξ [12]. It is then assumed that when this sensor is above a given level, the resolved flame wrinkling (seen from the dynamics of the resolved gradient) is large enough so that some unresolved flame wrinkling must exist within the subgrid. Power laws have been reported in the literature to express Ξ [12,13],

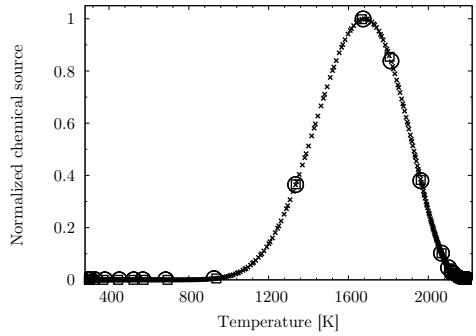

Figure 3: Chemical source in a freely propagating premixed flame. Simulation at the 5-th order. x: $h = 15\mu\text{m}$. Circle: $898\mu\text{m}$. Square: $1795\mu\text{m}$.

with a scaling for its maximum level derived from fractal analysis $\Xi_{\text{max}} \approx (\Delta/\delta_{\text{c}})^{\beta}$ [14, 15], where Δ is here an estimation of the LES filter size, δ_{c} is a cut-off length scale and β a parameter to be adjusted. Based on $s_{\nabla Y}$ the gradient sensor, Ξ is allowed to evolve dynamically in the simulation between unity and Ξ_{max}: $\Xi(s_{\nabla Y}(\underline{x},t)) = 1 + \alpha(s_{\nabla Y}(\underline{x},t))\,(\Xi_{\text{max}} - 1)$, with $\alpha(s_{\nabla Y}(\underline{x},t)) = 0.5\,(1 + \tanh(s_{\nabla Y}(\underline{x},t) + a) \times b)$ (a = 11.5 and b = 15.0). The source term and the diffusive budget are then amplified by Ξ to account for SGS flame wrinkling. In an additional simulation it is also tempted to apply Ξ to the chemical source only.

Table 1: Response versus mesh resolution and order of accuracy of: δ the mean distance between the solution points; S_L the flame speed; n_s the number of points within the flame profile and F^{o} the global thickening factor.

Element size h	Order $n = p + 1$	δ h/p [µm]	S_L [cm · s^{-1}]	n_s $\delta_{\text{Th}}/\delta + 1$	F^{o} $\delta_{\text{Th}}/\delta^{\text{o}}_{\text{Th}}$
898µm	5	224	40.4	5	4.6
	7	150	39.9	4	2.2
	9	112	39.7	4	1.9
1795µm	5	359	40.3	4	9.5
	7	299	40.5	4	4.5
	9	224	41.9	4	2.9

3 Application to freely propagating laminar flame and three-dimensional turbulent flame

The temperature profiles in a freely propagating flame simulated with single-step chemistry are shown in Fig. 2 for the three meshes of Table 1, plus a fully resolved flame. The method manages to thicken the flame so that the signal is sufficiently resolved to propagate at the expected speed for all meshes and order of accuracy. In Fig. 3, the chemical source normalised by its maximum value is plotted versus temperature, thus in composition space. The refined and reference simulation ($h = 15\mu\text{m}$) is shown along with the $h = 898\mu\text{m}$ and the $h = 1795\mu\text{m}$ solutions for the 5th order of accuracy. The method automatically distributes the burning rate signal over 4 points according to the resolution. Notice that between these points, the solution benefits from the fact that it is represented by a $p = 4$-th order polynomial approximation ($n = 5 = p + 1$).

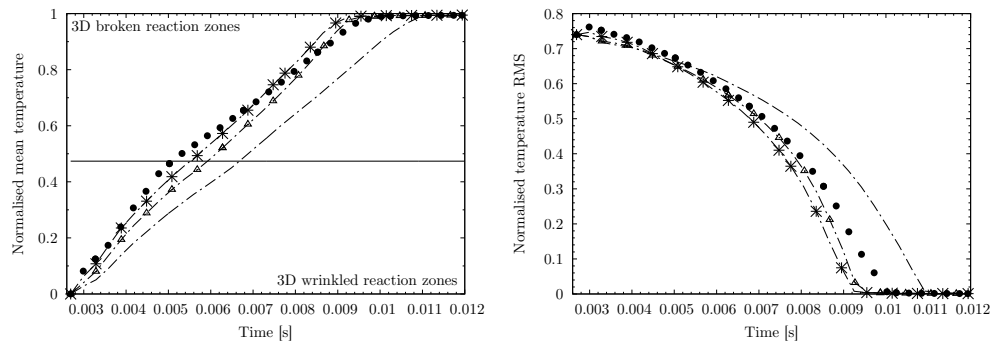

(a) $\langle T \rangle^+$ (b) $\sqrt{T_{\rm v}^+}$

Figure 4: Three dimensional turbulence. •: $\delta = h/p = 150\mu\text{m}$. Dot-dashed-line: $\delta = 299\mu\text{m}$. Line with no-symbol: $\Xi = 1$. Line with-symbols: Ξ by modal analysis. Triangle: $\beta = 1$. Star: Ξ on source term only with $\beta = 1$ and $\delta_c = 0.8\delta^o_{\rm th}$.

Two planar turbulent flames propagating toward each other and interacting with isotropic turbulence is now simulated. In the turbulent flow generated from Taylor Green Vortices [16], the enstrophy reaches its maximum $\mathcal{E}_{\rm max}$, there the flame simulation starts with a level of turbulent kinetic energy $k = 18.37\text{m}^2 \cdot \text{s}^{-2}$. The ratio of characteristic velocity fluctuations to the laminar flame speed is $k^{1/2}/S_{\rm L} = 10$, the turbulent Reynolds number is $Re_T = k^{1/2}\ell_T/\nu = 2174$, the Karlovitz number is $Ka = \tau_{\rm c}/\tau_k = 11$ and the Damköhler number is $Da = \tau_{\rm c}/\tau_{\rm T} = Re_{\rm T}^{1/2}/Ka = 4.26$, where the chemical time is based on the ratio $\tau_{\rm c} = \delta^{\rm o}_{\rm Th}/S_{\rm L} = 0.49$ms. The Kolmogorov time is $\tau_k = (1/2\mathcal{E}_{\rm max})^{1/2} = 64\mu$s, the eddy turn over time is $\tau_{\rm T} = k^{1/2}/(4\nu\mathcal{E}_{\rm max}) = 2.1$ms, the integral length scale is $\ell_T = 45\delta^{\rm o}_{\rm Th} = 9$mm and the expected smallest length scales in the flow are of the order of $\eta_k = 28\mu\text{m}$. At start, the turbulent flame is thus expected to evolve in the wrinkled flamelet regime. DNS is usually reached for a resolution of $2\times\eta_k$ so here $\delta_{\rm DNS} = 56\mu\text{m}$ [17], therefore the mesh with $\delta = h/p = 150\mu\text{m} = 2.68\delta_{\rm DNS}$, already provides a quite good resolution for both the flow and the flame ($\delta_{\rm Th} = 200\mu\text{m}$). In this reference simulation ($\delta = 150\mu\text{m}$), the modeling based on modal analysis leads to $\Xi = 1$ and $D_{\rm Add} \simeq 0$.

Figure 4 shows the time evolution of the statistical mean of the temperature and its variance in the domain. The solution on a coarser mesh ($h = 299\mu\text{m}$) is quite close to the refined one. In theory, a perfect modelling should report the same statistical results whatever the mesh and this constitutes a quite stringent test of SGS modeling. The growth rate of the volume of burnt gases produced by the turbulent flames is well captured in Fig. 4. It is also seen that the determination of Ξ by the modal analysis improves the results compared to using a fixed value.

References

[1] O. Colin, F. Ducros, D. Veynante, and T. Poinsot. A thickened flame model for Large Eddy Simulations of turbulent premixed combustion. *Physics of Fluids*, 12(7):1843–1863, 2000.

[2] D.A. Kopriva and J.H. Kolias. A conservative staggered-grid Chebyshev multidomain method for compressible flows. *J. Comput. Phys.*, 125(1):244–261, 1996.

[3] Y. Sun, Z.J. Wang, and Y. Liu. High-order multidomain spectral difference method for the Navier-Stokes equations on unstructured hexahedral grids. *Commun. Comput. Phys.*, 2(2):310–333, 2007.

[4] A. Jameson. A proof of the stability of the spectral difference method for all orders of accuracy. *J. Sci. Comput.*, 45(1):348–358, 2010.

[5] H.T. Huynh. A flux reconstruction approach to high-order schemes including discontinuous Galerkin methods. *AIAA P.*, 2007-4079:1–42, 2007. 18th AIAA Computational Fluid Dynamics Conference, Miami, FL, Jun. 25–28, 2007.

[6] H.T. Huynh. A reconstruction approach to high-order schemes including discontinuous Galerkin for diffusion. *AIAA P.*, 2009-403:1–34, 2009. 47th AIAA Aerospace Sciences Meeting, Orlando, FL, Jan. 5–8, 2009.

[7] P.E. Vincent, P. Castonguay, and A. Jameson. A new class of high-order energy stable flux reconstruction schemes. *J. Sci. Comput.*, 47(1):1–23, 2010.

[8] G. Lodato, L. Vervisch, and P. Clavin. Direct numerical simulation of shock wavy-wall interaction: analysis of cellular shock structures and flow patterns. *J. Fluid Mech.*, 789:221–258, 2016.

[9] Jan S. Hesthaven and Tim Warburton. *Nodal Discontinuous Galerkin Methods: Algorithms, Analysis, and Applications*. Springer Science & Business Media, LLC, 2008.

[10] P.-O. Persson and J. Peraire. Sub-cell shock capturing for Discontinuous Galerkin methods. In *American Institute of Aeronautics and Astronautics*, volume 2006-112, pages 1–13, 2006. 44th AIAA Aerospace Sciences Meeting and Exhibit, Reno, NV, Jan. 9–12.

[11] P. O. Persson. Shock capturing for high-order Discontinuous Galerkin simulation of transient flow problems. In *American Institute of Aeronautics and Astronautics*, volume 2013-3061, 2013. 21st AIAA Computational Fluid Dynamics Conference, San Diego, CA, Jun. 24–27.

[12] G. Wang, M. Boileau, and D. Veynante. Implementation of a dynamic thickened flame model for Large Eddy Simulations of turbulent premixed flames. *Combust. Flame*, 158(11):2199–2213, 2011.

[13] F. Charlette, C. Meneveau, and D. Veynante. A power-law flame wrinkling model for LES of premixed turbulent combustion Part I: non-dynamic formulation. *Combust. Flame*, 131(1-2):159–180, 2002.

[14] F. C. Gouldin, K.N.C. Bray, and J.-Y. Chen. Chemical closure model for fractal flamelets. *Combust. Flame*, 77(3-4):241–259, 1989.

[15] O. L. Gülder. Turbulent premixed combustion modelling using fractal geometry. *Symposium (Int) on Combustion*, 23(1):835–842, 1991.

[16] M. Brachet, D. Meiron, S. Orszag, B. Nickel, R. Morf, and U. Frisch. Small-scale structure of the taylor-green vortex. *J. Fluid Mech.*, 130(41):411–452, 1983.

[17] P. Moin and K. Mahesh. Direct numerical simulation: A tool in turbulence research. *Annu. Rev. Fluid Mech.*, 30:539–578, 1998.